1521-0111/12/8204-623–635$25.00
MOLECULAR PHARMACOLOGY
Copyright © 2012 The American Society for Pharmacology and Experimental Therapeutics
Mol Pharmacol 82:623–635, 2012

Vol. 82, No. 4
78220/3793121

MOL PHARM

RNA Aptamer-Based Functional Ligands of the Neurotrophin Receptor, TrkB

Yang Zhong Huang, Frank J. Hernandez, Bin Gu, Katie R. Stockdale, Kishore Nanapaneni, Todd E. Scheetz, Mark A. Behlke, Andrew S. Peek, Thomas Bair, Paloma H. Giangrande, and James O. McNamara II

Department of Neurobiology (Y.Z.H.) and Department of Pharmacology and Cancer Biology (B.G.), Duke University Medical Center, Duke University, Durham, North Carolina; Department of Internal Medicine (F.J.H., K.R.S., P.H.G., J.O.M.), Center for Bioinformatics and Computational Biology (K.N., T.E.S.), Department of Biomedical Engineering (K.N., T.E.S.), and Department of Ophthalmology and Visual Sciences (T.E.S.), Roy J. and Lucille A. Carver College of Medicine, University of Iowa, Iowa City, Iowa; Integrated DNA Technologies, Coralville, Iowa (M.A.B., A.S.P.); and DNA Facility, University of Iowa, Iowa City, Iowa (T.B.)

Received February 9, 2012; accepted June 29, 2012

ABSTRACT

Many cell surface signaling receptors, such as the neurotrophin receptor, TrkB, have emerged as potential therapeutic targets for diverse diseases. Reduced activation of TrkB in particular is thought to contribute to neurodegenerative diseases. Unfortunately, development of therapeutic reagents that selectively activate particular cell surface receptors such as TrkB has proven challenging. Like many cell surface signaling receptors, TrkB is internalized upon activation; in this proof-of-concept study, we exploited this fact to isolate a pool of nuclease-stabilized RNA aptamers enriched for TrkB agonists. One of the selected aptamers, C4-3, was characterized with recombinant protein-binding assays, cell-based signaling and functional assays, and, in vivo in a seizure model in mice. C4-3 binds the extracellular domain of TrkB with high affinity (K_D ~2 nM) and exhibits potent TrkB partial agonistic activity and neuroprotective effects in cultured cortical neurons. In mice, C4-3 activates TrkB upon infusion into the hippocampus; systemic administration of C4-3 potentiates kainic acid-induced seizure development. We conclude that C4-3 is a potentially useful therapeutic agent for neurodegenerative diseases in which reduced TrkB activation has been implicated. We anticipate that the cell-based aptamer selection approach used here will be broadly applicable to the identification of aptamer-based agonists for a variety of cell-surface signaling receptors.

Introduction

Signaling via the neurotrophin receptor, TrkB, is critical to diverse biological processes in the central nervous system (CNS), including neuronal survival and differentiation as well as synaptic structure, function, and plasticity. TrkB is widely expressed in the developing and mature mammalian CNS. The prototypic neurotrophin ligands of TrkB, brain-derived neurotrophic factor (BDNF), and neurotrophin-4, are 14-kDa proteins that are packed and released from dense core vesicles of nerve terminals. The binding of BDNF to the TrkB extracellular domain (ECD) induces receptor dimerization and subsequent phosphorylation of tyrosine residues within the intracellular domain, thereby initiating downstream signaling, including mitogen-activated protein kinase and phospholipase-Cγ pathways (Huang and Reichardt, 2001).

Dysregulation of TrkB signaling has been implicated in the pathogenesis of several CNS disorders, including neurode-

This work was supported by the National Institutes of Health National Institute of Neurological Disorders and Stroke [Grant NS056217]; and by a postdoctoral fellowship from the American Heart Association (to F.J.H.).

Duke University (B.G. and Y.Z.H.) and the University of Iowa (J.O.M., F.J.H., and P.H.G.) have applied for a patent on this technology. M.A.B. is employed by Integrated DNA Technologies, Inc. (IDT), which offers oligonucleotides for sale that are similar to some of the compounds described in the article. IDT, however, is not a publicly traded company, and M.A.B. does not personally own any shares/equity in IDT.

Article, publication date, and citation information can be found at http://molpharm.aspetjournals.org.

http://dx.doi.org/10.1124/mol.112.078220.

ABBREVIATIONS: CNS, central nervous system; BDNF, brain-derived neurotrophic factor; ECD, extracellular domain; SELEX, systematic evolution of ligands by exponential enrichment; E18, embryonic day 18; HEK, human embryonic kidney; PCR, polymerase chain reaction; DPBS, Dulbecco's phosphate-buffered saline; SPR, surface plasmon resonance; BSA, bovine serum albumin; PAGE polyacrylamide gel electrophoresis; p, phospho; FAM, fluorescein amidite; FITC, fluorescein isothiocyanate; LDH, lactate dehydrogenase; KA, kainic acid; AP, anteroposterior; ML, mediolateral; DV, dorsoventral; PBS, phosphate-buffered saline; EEG, electroencephalogram; shRNA, short hairpin RNA; Scr, scrambled; ANOVA, analysis of variance; MK-801, 5*H*-dibenzo[*a*,*d*]cyclohepten-5,10-imine; RTK, receptor tyrosine kinase.

MOLECULAR PHARMACOLOGY
aspet
Downloaded from molpharm.aspetjournals.org at Universidade do Estado do Rio de Janeiro on December 1, 2012

MOL PHARM
MOLECULAR PHARMACOLOGY
aspet

generative diseases. The expression of BDNF and activation of TrkB in cortical neurons is reduced in striatal neurons in Huntington's disease (Zuccato et al., 2001). Reduced BDNF protein levels were also found in the entorhinal cortex and hippocampus in humans with Alzheimer's disease (Zuccato and Cattaneo, 2009). Of importance, supplementing BDNF levels in the brain by viral expression reverses neural atrophy and ameliorates cognitive impairment in rodent and primate models of Alzheimer's disease (Nagahara et al., 2009). Thus, enhancing activation of TrkB may limit neuronal degeneration and progression of some neurodegenerative diseases. However, excessive activation of TrkB is also sufficient to induce both epilepsy and neuropathic pain (Croll et al., 1999; Lahteinen et al., 2003; Coull et al., 2005; Hu and Russek, 2008; He et al., 2010). Ligands used to enhance TrkB activation for therapeutic purposes therefore must not excessively activate this receptor.

Partial agonists are one type of receptor ligand that is particularly well suited to address this problem. A partial agonist is a receptor ligand that elicits a submaximal level of receptor activation compared with that elicited by a full agonist. Thus, the features of a partial agonist may tilt the balance of TrkB signaling to a level with a beneficial effect yet prevent excessive activation of TrkB. Indeed, several partial agonists of neuronal receptors are clinically effective drugs including buspirone (serotonin 5-HT_{1A} receptor anxiety) (Robinson et al., 1990) and varenicline ($\alpha_4\beta_2$ nicotinic cholinergic receptor for smoking cessation) (Jorenby et al., 2006). Partial agonists for TrkB have not been described.

RNA aptamers (synthetic, structural RNAs), which typically bind a target protein with high affinity and specificity, are emerging as a novel class of therapeutic reagents with a variety of uses including anticoagulation and targeted therapeutic delivery (Keefe et al., 2010). One of the most intriguing features of RNA aptamer technology is that the aptamer identification process known as systematic evolution of ligands by exponential enrichment (SELEX) provides a versatile ligand discovery platform that can be tailored to enrich for receptor ligands with diverse *functional* properties. Thus, we hypothesized that we could identify RNA aptamers that serve as partial agonists of TrkB.

Here we describe a novel, functional cell-based SELEX approach for the identification of TrkB agonists in mammalian cells. We identified a TrkB ECD-binding RNA aptamer that exhibits partial agonistic activity in cultured neurons and upon infusion into the mouse hippocampus in vivo, yet was also capable of limiting BDNF-mediated activation of TrkB.

Materials and Methods

Reagents. BDNF was purchased from Millipore Bioscience Research Reagents (Temecula, CA). Other reagents were obtained from Sigma-Aldrich (St. Louis, MO) unless specified otherwise. The full-length TrkB mammalian expression plasmid pcDNA3-FLAG-TrkB was described previously (Huang and McNamara, 2010).

Cell Culture and Transfection. Cortical neuron/glia mixed cultures were prepared from embryonic day 18 (E18) pups of pregnant Sprague-Dawley rats (Charles River Laboratories, Inc., Wilmington, MA) as described previously (Huang et al., 2008). The neurons were cultured in Neurobasal with B27 supplement and GlutaMAX (Invitrogen, Carlsbad, CA) for 12 to 24 days in vitro. HEK293 cells were maintained in Dulbecco's modified Eagle's medium supplemented with 10% fetal bovine serum. For plasmid DNA transfection, HEK293 cells were plated 12 h before transfection at a density of 5×10^5 cells/well of a six-well culture plate and were transfected using the Lipofectamine method (Invitrogen). Twenty-four hours after transfection, G418 (1 mg/ml) was added to the medium for 14 days. A single-cell clone was selected and expanded. Animals were handled according to the National Institutes of Health *Guide for the Care and Use of Laboratory Animals* (Institute of Laboratory Animal Resources, 1996) and approved by Duke University Animal Welfare Committee.

Cell Internalization SELEX. An RNA library consisting of 2′-fluoro pyrimidine-modified RNAs, 51 nucleotides long with a central, 20-nucleotide variable region, was prepared as described previously (McNamara et al., 2008). For library preparation, a template DNA oligo (5′-TCGGGCGAGTCGTCTGNNNNNNNNNNNNNNNNNNCCGCATCGTCCTCCC-3′) and a 5′-oligo (5′-TAATACGACTCACTATAGGGAGGACGATGCGG) (both synthesized by Integrated DNA Technologies, Coralville, IA) were annealed and extended with Taq polymerase (Denville Scientific Inc., Metuchen, NJ). The resulting duplex was used as a template for in vitro transcription with a mutant (Y639F) T7 RNA polymerase and the following nucleotide triphosphates: 1 mM ATP (Roche Diagnostics, Indianapolis, IN), 1 mM GTP (Roche Diagnostics), 3 mM 2′-fluoro-CTP (TriLink BioTechnologies, San Diego, CA), and 3 mM 2′-fluoro-UTP (TriLink). Full-length RNA was gel-purified on a denaturing urea-acrylamide gel (RNA was visualized with UV shadowing), and 10% of the RNA recovered from cells after each cell-internalization procedure (outlined below) was reverse-transcribed with a 3′-oligo (5′-TCGGGCGAGTCGTCTG-3′) (Integrated DNA Technologies) using AMV reverse transcriptase (Roche Diagnostics); the reverse transcriptase reaction was then used as template in a 1-ml, 20-cycle PCR with 5′-oligo and 3′-oligo to generate the transcription template for the subsequent round of selection.

For the first round, 750 pmol of library RNA were used; 500 pmol of RNA were used in each subsequent round. The procedure for each round was as follows. A 150-mm dish of HEK cells (~90% confluent) was first blocked by washing the cells twice with Dulbecco's phosphate-buffered saline (DPBS) containing calcium and magnesium (Invitrogen) followed by incubation at 37°C for 15 min in 15 ml of DPBS supplemented with 100 μg/ml yeast tRNA (Invitrogen).

To "preclear" the library, the DPBS/tRNA was replaced with 15 ml of DPBS containing the library and 100 μg/ml yeast tRNA. After a 15-min incubation at 37°C, the supernatant was transferred to a centrifuge tube and spun at 2500 rpm in a table-top centrifuge to pellet cellular debris. After centrifugation, the supernatant was transferred to a 150-mm dish of TrkB-expressing HEK cells (~90% confluent) that had been blocked with tRNA as described for the HEK cells above. After a 20-min incubation at 37°C, with periodic gentle mixing, the supernatant was discarded. The cells were washed once with ice-cold DPBS and once with ice-cold 0.5 M NaCl and then were incubated at 4°C for 5 min in 20 ml of ice-cold 0.5 M NaCl. After the 0.5 M NaCl was discarded, cells were washed once with DPBS, and then total RNA was purified from the cells with TRIzol (Invitrogen) extraction. TRIzol extraction proceeded as outlined by the manufacturer except that 2 μl of 5 mg/ml linear acrylamide (Ambion, Austin, TX) was added to each aqueous phase (after chloroform addition) to facilitate RNA precipitation. The RNA pellet obtained from the TRIzol procedure was suspended in 600 μl of DPBS. The endogenous RNA was then digested at 37°C for 25 min after addition of 6 μl of RNase A (Fermentas; Thermo Fisher Scientific, Waltham, MA). RNA was then purified with phenol-chloroform-isoamyl alcohol and chloroform extractions, followed by ethanol precipitation. Each dried RNA pellet was dissolved in 50 μl of water and stored at −20°C. A similar "preclearing" strategy was implemented for each subsequent round of selection.

454 Sequencing of the Round 4 PCR Product. The round 4 PCR product (1.1 μM DNA duplex concentration) was diluted 1:100 with water, and 1 μl of this was used as template for a 20-cycle,

Downloaded from molpharm.aspetjournals.org at Universidade do Estado do Rio de Janeiro on December 1, 2012

MOL PHARM

MOLECULAR PHARMACOLOGY

100-μl PCR with the following primers (synthesized by Integrated DNA Technologies): primer A.8 (5′-GCCTCCCTCGCGCCATCAG-*GTCAGTCAAT*TAATACGACTCACTATAG) and primer B (5′-GCCTTGCCAGCCCGCTCAGTCGGGCGAGTCGTCTG). The 3′ portions of each primer provided annealing (amplification) sites for the round 4 DNA duplex, whereas the 5′ portions provided annealing sites for the 454 reaction. The underlined portion of primer A.8 was used as a bar code, which allowed the inclusion of multiple, distinct PCR products in the 454 reaction. The PCR product was purified with a Miniprep column (QIAGEN, Valencia, CA) and then combined with PCR products generated in the same manner (but with distinct bar codes) and submitted to the University of Minnesota sequencing facility. Sequences were clustered as described previously (Scheetz et al., 2005).

Computational Comparison of Predicted Aptamer Secondary Structures. The most stable secondary structure of each unique aptamer sequence identified from the TrkB selection round 4 PCR product was predicted with the Vienna RNA Package Secondary Structure Prediction algorithm, version 2.0. This algorithm predicts RNA secondary structures on the basis of an energy minimization algorithm. The structural similarities (tree distances) of the predicted structures were also computed with the Vienna RNA Package and then output was written to a file that enabled graphical representation of the relationships with Cytoscape.

TrkB-SPR Measurements. All measurements were performed with a Biacore 3000 at 37°C in DPBS running buffer (0.901 mM calcium chloride, 0.493 mM magnesium chloride, 2.67 mM potassium chloride, 1.47 mM potassium phosphate monobasic, 137.93 mM sodium chloride, and 8.06 mM sodium phosphate dibasic). Immobilization of ligands to CM5 and SA chips (GE Healthcare, Chalfont St. Giles, Buckinghamshire, UK) followed standard procedures recommended by the manufacturer and protocols described previously (Hernandez et al., 2009a,b).

SELEX Round SPR measurements. The recombinant mouse TrkB extracellular domain (R&D Systems, Minneapolis, MN) was immobilized on a CM5 sensor chip by amine coupling. Next, BDNF was injected at concentrations ranging from 10 to 100 nM to confirm the functionality of the immobilized TrkB protein. The SELEX rounds were assessed by injecting 2.5 μM concentrations of each RNA pool at a flow rate of 15 μl/min. Finally, the signals were aligned by BIAevaluation 4.1 software.

Determination of C4-3 Affinity for TrkB. Immobilization of the C4-3 aptamer was performed by the streptavidin-biotin coupling method. C4-3 aptamer was previously biotinylated at the 3′ end by periodate oxidation as described previously (Qin and Pyle 1999). The flow rate was set to 5 μl/min, and the biotinylated C4-3 was injected at a concentration of 1 μM over the streptavidin surface (SA sensor chip) for 15 min at 25°C. The unbound aptamer was removed by treatment with 50 mM aqueous NaOH, and the chip was primed before use. TrkB protein solutions were sequentially injected over the sensor surface for 3 min at 15 μl/min with a 3-min dissociation time. Six concentrations of TrkB protein were injected by serially diluting samples from 400 to 12.5 nM. The selectivity studies were performed by injecting 200 nM bovine serum albumin (BSA) and 200 nM TrkB protein over the C4-3 aptamer and a control aptamer (4-1BB). The immobilization and injections for these control samples were performed under the same conditions described above. After each run, the surface was regenerated with 50 mM aqueous NaOH for 5 s at 15 μl/min. The raw data were processed and analyzed to determine the binding constant for C4-3 aptamer. To correct for refractive index changes and instrument noise, the response of the control surface data was subtracted from the responses obtained from the reaction surface using BIAevaluation software 4.1. The K_D was calculated by global fitting of the six concentrations of TrkB protein, assuming a constant density of C4-3 aptamer on the surface. A 1:1 binding mode with mass transfer fitting was used to obtain the kinetic data. BSA and 4-1BB aptamer measurements were aligned to the C4-3 aptamer and TrkB data for nonspecific analysis.

Western Blotting. Cultured neurons or HEK293 cells were lysed in modified radioimmunoprecipitation assay buffer (10 mM Tris · HCl, pH 7.4, 1% Triton X-100, 0.1% sodium deoxycholate, 3 mM Na_3VO_4, 1 mM EDTA, and protease inhibitors) and centrifuged at 16,000*g* for 10 min; the supernatant was defined as cell lysate. Mouse hippocampus was homogenized in a buffer containing 4 mM HEPES and 0.32 M sucrose, pH 7.4. Cell lysates (10–20 μg) or homogenates were resolved by SDS-PAGE. The blots were incubated overnight with primary antibodies and subsequently with secondary antibodies (1:5000) for 1 h at room temperature. The antibodies and dilution used in this study are as follows: p-Trk (pY515), p-Trk (pY705/706), p-Src (Y416), p-Akt, and p-Erk (1:1000; Cell Signaling Technology, Danvers, MA); TrkB (1:500; BD Transduction Laboratories, Lexington, KY); and β-actin (1:10,000; Sigma-Aldrich). p-TrkB (pY816) (1:1000) was kindly provided by Dr. Moses Chao (New York University, New York, NY). The immunoblots were developed with enhanced chemiluminescence (GE Healthcare). An equivalent amount of protein loaded in each lane was verified with immunoblotting with antibodies to TrkB or actin. Immunoblots were scanned with a digital scanner, and optical band density was quantified with ImageJ analysis software. Optical densities were normalized to actin levels. Data are presented as mean ± S.E.M. Results shown are representative of at least three independent immunoblotting experiments.

Fluorescence Microscopy: Localization of C4-3 on HEK Cells. HEK cells and HEK cells expressing TrkB were grown on 35-mm glass-bottom MatTek culture dishes in Dulbecco's modified Eagle's medium supplemented with 10% fetal bovine serum overnight. Cells were washed with prewarmed DPBS and incubated for 1 h at 37°C with FAM-labeled (FAM was on the 3′ end) C4-3 or control aptamer (100 μl of 100 nM RNA) diluted in DPBS. Control aptamer (5′-GGGAGGACGAUGCGGUUUGGGGUUUUCCCGUGCCCCAGACGACUCGCCCGA-3′) has identical modifications (2′-fluoro-modified pyrimidines) and fixed region sequences as C4-3, but a different variable region (underlined above). Next, cells were washed twice with ice-cold DPBS followed by a 5-min wash with 0.5 M NaCl and 0.2 N acetic acid at 4°C to remove unbound and surface-bound RNAs. Cells were then fixed with 4% formaldehyde and 4% sucrose in DPBS for 20 min at room temperature. After fixation, the cells were permeabilized with 0.1% Triton X-100 in DPBS for 5 min and then incubated in block (5% goat serum plus 0.1% Triton X-100 in DPBS) for 1 h at room temperature. The fluorescence signal of the FAM tag was enhanced by incubation with an anti-FITC antibody (rabbit anti-FITC, 1:1000 dilution; Invitrogen) followed by a fluorescent secondary antibody (goat anti-rabbit IgG, Alexa Fluor 488 conjugate, 1:1000 dilution; Invitrogen). After labeling, cells were mounted with a glycerol mounting medium and a coverslip. Images of internalized aptamers were acquired with a 40× oil immersion objective on an Olympus IX71 inverted microscope equipped with a cooled charge-coupled device camera and filters for FITC (excitation, 450–490 nm; emission, 515–565 nm). The fluorescence images shown are representative of at least three captured images per condition.

Cell Death Assay. Cell death was assessed by measuring lactate dehydrogenase (LDH) activity in culture supernatants by a spectrophotometric method (Whitney and McNamara, 2000). Data are presented as the means ± S.E.M. of determinations made in six wells per condition from four independent experiments.

Hippocampal Interstitial Infusion. Animals were handled according to the National Institutes of Health *Guide for the Care and Use of Laboratory Animals* and approved by the Duke University Animal Care and Welfare Committee. Adult mice were anesthetized with isoflurane (5% induction; 1.5% maintenance) and mounted in a stereotaxic apparatus. The skull was exposed, and a hole was drilled over the hippocampus (−2.5 mm AP and 2.2 mm ML). A 30-gauge infusion cannula (Plastics One, Inc., Roanoke, VA) connected to a Hamilton syringe (Hamilton Co., Reno, NV) via plastic tubing, was lowered into the hippocampus (1.8 mm DV), and vehicle or scrambled or C4-3 aptamer was infused into the hippocampus at a flow rate of

Downloaded from molpharm.aspetjournals.org at Universidade do Estado do Rio de Janeiro on December 1, 2012

MOL PHARM

MOLECULAR PHARMACOLOGY

0.1 μl/min over a period of 20 min using a calibrated syringe pump (Harvard Apparatus Inc., Holliston, MA). Animals were sacrificed 30 min after the start of the infusion, brains were removed, and hippocampus was isolated.

KA Amygdala Infusion. Continuous limbic and tonic-clonic seizures (status epilepticus) were induced in awake, adult male wild-type C57BL/6 mice (Mouri et al., 2008) weighing 20 to 25 g by stereotaxic microinjection of 0.3 μg of KA (Sigma-Aldrich) in a 0.5-μl volume of PBS, pH 7.4, at 0.11 μl/min into the right basolateral amygdala nucleus through a guide cannula (Plastics One, Inc.). At least 7 days before infusion of KA, the guide cannula was implanted in the right amygdala under pentobarbital anesthesia using the following stereotaxic coordinates relative to bregma (AP, −0.94 mm; ML, +2.85 mm; and DV, −3.75 mm); in addition, a bipolar EEG recording electrode was placed into the left dorsal hippocampus (−2.00 mm AP; −1.60 mm ML; and −1.53 mm DV). Either PBS or scrambled (Scr) aptamer or C4-3 aptamer (200 nmol/kg) was injected intravenously through the tail vein 15 min before KA infusion. EEG and behavior were monitored by an EEG recording device (Grass Technologies, Inc., West Warwick, RI) and video camera (Victor Company of Japan, Ltd., Yokohama, Japan), respectively, for 45 min after infusion. EEG status epilepticus was defined as continuous electrographic seizures (including postictal depression and or polyspikes).

Scoring of Behavioral Seizures. Behavioral seizures were scored on the basis of the modified Racine scale (Racine, 1972): in detail, class 0, normal behavior; class 1, behavioral arrest and rigid posture (with or without extended tail); class 2, head bobbing; class 3, unilateral forelimb clonus and bilateral forelimb clonus without rearing; class 4, rearing and bilateral forelimb clonus; class 5, rearing and falling, loss of posture; and class 6, running and jumping.

Statistical Analysis. Data are presented as means ± S.E.M. In KA amygdala infusion experiments, the PBS and Scr-aptamer groups were combined into a single control group because of the absence of a significant difference between them (Student's t test or the Mann-Whitney U test; $p > 0.05$). Statistical significance was assessed with the Mann-Whitney U test or one-way ANOVA post hoc t tests unless noted otherwise.

Results

Internalization-Based Screen for TrkB-Specific Aptamers. The mechanism of activation of TrkB has been well studied. The external signals that mediate activation of TrkB are neurotrophins including BDNF and NT4, 14-kDa proteins packed in the dense-core vesicle of nerve terminals. BDNF binds to the ECD of TrkB and induces receptor dimerization, leading to autophosphorylation of tyrosines within the intracellular domain and subsequent initiation of downstream signaling pathways. Once activated, surface TrkB is internalized into intracellular compartments. To search for RNA aptamers that activate TrkB, we sought to isolate RNAs bound to and subsequently internalized with murine TrkB expressed in mammalian cells. The initial step was to establish a mammalian cell line stably expressing TrkB. Toward that end, HEK293 cells were transiently transfected with a plasmid expressing murine TrkB. A single colony of G418-resistant and TrkB-expressing HEK cells was then selected. The presence of TrkB on the HEK cell surface was verified with immunofluorescence (Fig. 1B). Of importance, incubation of TrkB-expressing HEK cells with BDNF (10 ng/ml for 15 min) resulted in TrkB activation as evidenced by increased phosphorylation of TrkB and Erk mitogen-activated protein kinase, a signaling protein downstream of TrkB (Fig. 1C).

This TrkB-HEK cell line was subsequently used to select for RNA aptamers that bind TrkB. To reduce the presence of aptamers that bind molecules expressed on the surface of HEK cells other than TrkB, the RNA library was "precleared" by incubation with HEK cells lacking TrkB (Fig. 1A; *Materials and Methods*). After preclearing, the supernatant containing the RNA library was incubated with TrkB-expressing HEK cells, and RNA internalized by these cells was recovered and amplified by PCR, and the procedure was repeated.

Identification of TrkB Aptamers by High-Throughput Sequencing. A 51-nucleotide, 2′-fluoro pyrimidine-modified RNA library was used for the selection. After four rounds, the ability of the RNA pools to bind the ECD of recombinant murine TrkB was measured with surface plasmon resonance. The selected RNA pools exhibited progressive increases in binding to TrkB, with the round 4 pool exhibiting the greatest binding (Fig. 1D), implying an enrichment of TrkB-binding RNAs. The sequences of the round 4 aptamer pool were determined with the high-throughput 454 platform; a total of 7896 sequencing reads were obtained for this round.

Reads with identical variable regions were grouped into clusters. The number of reads per cluster ranged from 1 to 8, with most clusters consisting of a single read (Fig. 2A). The secondary structures of the RNA sequences were also predicted and compared. A graphical representation of the predicted structural similarity of the RNA sequences is shown in Fig. 2B. Each sequence was represented with a node, and nodes with related predicted structures were connected with lines. This analysis revealed the presence of many minimally related structural species (i.e., the nodes at the bottom of the figure), as well as two large groups of sequences with related structures. Several sequences were chosen from the largest clusters for further study (Table 1).

Selected Aptamers Activate TrkB Signaling in Cortical Neurons. To test whether the selected aptamers can activate TrkB, the tyrosine phosphorylation of TrkB was monitored in aptamer-treated primary cultures of embryonic rat cortical neurons. Selected aptamers were prepared by in vitro transcription and gel-purified. Cortical neurons were incubated with vehicle, BDNF (10 ng/ml), or selected aptamers (200 nM) for 15 min. Cell lysates were subjected to SDS-PAGE followed by immunoblotting with p-TrkB antibodies. BDNF induced an increase in phosphorylation of TrkB as well as downstream signaling molecules, Akt and Erk, providing a positive control for TrkB activation (Fig. 3A). Of interest, a subset of aptamers, including C4-2, C4-3, C4-6, C4-7, C5-2, and C5-3, was able to enhance the phosphorylation of TrkB, Akt, and Erk, indicating that these aptamers are TrkB agonists (Fig. 3A). In contrast, other aptamers, including C4-1, C4-4, C4-5, and C5-1 were inert in this assay (Fig. 3A and data not shown), thus indicating that the agonistic effects observed were not due to nonspecific effects of RNA application. These results demonstrate that RNA aptamers can function as agonists for TrkB.

C4-3 Binds to the Extracellular Domain of TrkB. The observation that a subset of the selected aptamers activates TrkB signaling in cultured neurons suggests that these aptamers bind directly to the ECD of TrkB. To test this possibility, we selected an aptamer with agonist properties, C4-3, for further study. Whereas the initial characterization of

Downloaded from molpharm.aspetjournals.org at Universidade do Estado do Rio de Janeiro on December 1, 2012

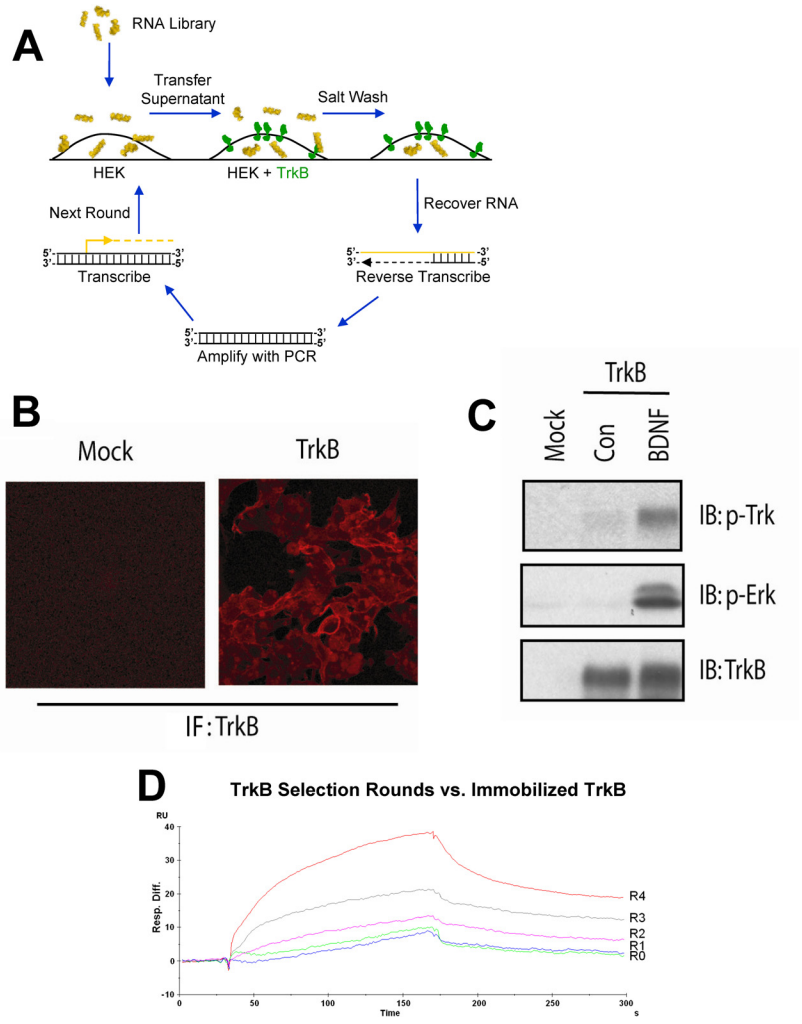

Fig. 1. Cell-based internalization SELEX for selection of TrkB agonistic aptamers. A, schematic of selection. B, characterization of TrkB stably transfected cells. HEK293 cells were transfected with either mock plasmid or TrkB-expressing plasmid pFLAG-TrkB. After incubation with G418 (1 mg/ml) for 14 days, a single-cell clone was selected. Mock-transfected or TrkB-transfected cells were fixed with 4% paraformaldehyde followed by a 12-h incubation with TrkB antibody at 4°C to label the portion of TrkB present on the cell surface; note that cells were not permeabilized when fixed. The anti-TrkB antibody was detected with a secondary antibody conjugated with Alexa Fluor 594 (red). Images shown are maximal projections of z-stack confocal images. C, BDNF activates TrkB in TrkB stable cells. TrkB cells were incubated with vehicle or BDNF (10 ng/ml) for 15 min. Cell lysates were resolved with SDS-PAGE. The expression of TrkB protein was detected with immunoblotting (IB) with an antibody specific to TrkB. The activation of Trk was revealed by probing the blots with antibodies to p-Trk and p-Erk. D, surface plasmon resonance analysis of binding of SELEX rounds to immobilized recombinant TrkB ECD. CON, control. IF, immunofluorescence; Resp. Diff, response difference.

C4-3 used enzymatically synthesized RNA, subsequent characterization was performed with chemically synthesized C4-3. Surface plasmon resonance was used to directly assess binding of C4-3 to the ECD of TrkB in a cell-free context. Application of BDNF to a sensor chip with immobilized, recombinant TrkB ECD resulted in concentration-dependent increases in resonance units, thus demonstrating the expected functionality of the recombinant TrkB ECD preparation (Fig. 4A). Application of the TrkB ECD to a sensor chip with immobilized C4-3 resulted in an increase of resonance units (Fig. 4B); the binding of C4-3 to TrkB ECD was specific because C4-3 did not bind a control protein, BSA (Fig. 4B). The fact that a control aptamer (M12-23, a 4-1BB-specific aptamer), also synthesized with 2′-fluoro-modified pyrimidines, failed to bind the TrkB ECD (Fig. 4C) indicates that the TrkB ECD is not a promiscuous binder of such chemically modified RNA. The binding of C4-3 to the TrkB ECD was a concentration-dependent and high-affinity interaction, with an equilibrium dissociation constant (K_d) of 2.1 nM (Fig. 4D). Taken together, these results demonstrate that C4-3 binds to the TrkB ECD in a cell-free system in vitro.

C4-3 Is Specifically Internalized by TrkB-Expressing HEK Cells. The fact that C4-3 was identified with a cell internalization selection suggests that C4-3 may be internalized upon binding to TrkB on the surface of cells. To explore this possibility, the localization of C4-3 was studied after incubation with TrkB-expressing or TrkB-negative HEK cells (Fig. 5). For this experiment, cells incubated for 1 h at 37°C with a FAM-labeled version of C4-3 (or a control sequence) were treated with a stringent wash to remove surface-bound RNA. Antibody-based detection of the FAM (after fixation and cell permeabilization) greatly improved the detection sensitivity of the internalized RNAs (K.R. Stockdale, unpublished observations). The C4-3 internalized by the TrkB-expressing cells (Fig. 5A) exhibited a punctate pattern, superimposed on a diffuse fluorescence pattern. Many of the puncta seemed to be adjacent to the plasma membrane, possibly indicating the presence of C4-3 in recycling endosomes. The diffuse fluorescence may be the result of a portion of the internalized C4-3 escaping from the endosomal compartment. The amount of C4-3 internalized by HEK cells that did not express TrkB was substantially less (Fig. 5B), thus indicating that the internalization of C4-3 seen in the TrkB-expressing cells is dependent on TrkB expression. The increased uptake of C4-3 by the TrkB-expressing cells was a C4-3-specific phenomenon because a control RNA sequence exhibited substantially less internalization into the TrkB-expressing cells (Fig. 5C). These observations are consistent with the conclusion that C4-3 binds the TrkB ECD on the cell surface and is subsequently internalized.

C4-3 Activates TrkB Signaling in Cultured Neurons. The observations that C4-3 binds directly to TrkB in a cell-

MOL PHARM
MOLECULAR PHARMACOLOGY
aspet
Downloaded from molpharm.aspetjournals.org at Universidade do Estado do Rio de Janeiro on December 1, 2012

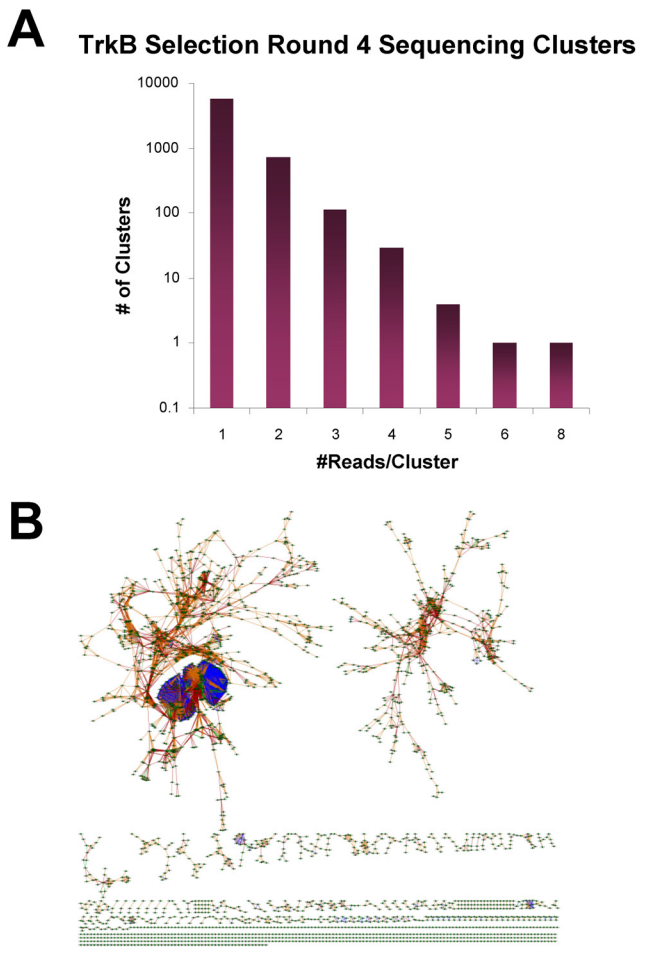

Fig. 2. Identification of TrkB aptamers with high throughput sequencing. A, Cluster analysis of 7896 sequencing reads obtained via 454 high throughput sequencing of the round 4 reverse transcription-PCR product. Although most sequences were read only one time, as indicated with the bar on the far left of the graph, several dozens of sequences were read three times or more. B, TrkB cell selection, round 4 sequence clusters, grouped by similarity of predicted secondary structure. The subset of the total pool of unique sequences (2805 of 6761) that was found to have related secondary structures is illustrated. Sequence clusters that do not have predicted structures with tree distances (a measure of predicted secondary structure similarity) of three or fewer to others within the pool are not illustrated. Each node represents an individual sequence cluster (i.e., a unique sequence). Blue lines indicate that the connected nodes have identical predicted secondary structures. Green, orange, and red lines indicate structures separated by tree distances of 1, 2, or 3, respectively. Blue thus indicates the greatest similarity and red indicates the least similarity in predicted secondary structure. A total of 445 families of sequences with related secondary structures were obtained. The largest and second largest families are illustrated in the upper left and upper right corners, respectively, of the figure, whereas the smallest families, consisting of pairs of nodes with related structures, are shown in the bottom of the figure.

free system as well as to native TrkB expressed on mammalian cells led us to further characterize the agonistic activity of this aptamer. Consistent with its binding affinity (K_D = ~2.1 nM), low nanomolar (2–20 nM) concentrations of C4-3 activated TrkB signaling in cultured cortical neurons as evidenced by enhanced phosphorylation of TrkB and Akt, a downstream signaling protein (Figs. 6A and 7A); C4-3 is thus a potent TrkB agonist. The activation of TrkB was specific to the sequence of C4-3 because a control aptamer with a scrambled variable region failed to enhance phosphorylation of TrkB (Fig. 6B), demonstrating the specificity of the agonistic

TABLE 1
Variable region sequences of aptamers from largest sequence clusters

Variable Region Sequence	Cluster Size	Name
UCCGAGACUCCACUCAUCGC	8	C8
CAUCACUCGGCACAUCGCGU	6	C6
CAUAAGACCGCUGCUUGCCC	5	C5-1
UUAAACCUUCAGUCUUUGUG	5	C5-2
CGUUACUCGACUCCCCGUAU	5	C5-3
CCGGAUCUAUCCCUACACAU	5	C5-4
UUCCAGAUCUACCGCGCCUG	4	C4-1
CAACAUCCAGACUGGGACGU	4	C4-2
UCGUAUUAUCCGCUGCACGC	4	C4-3
GACACCAGUCAGGUCUUGGU	4	C4-4
UACACCGUACGUAUUUUCGC	4	C4-5
UAAAUCGGGCUCUAACGUGU	4	C4-6
UCCUGAACAAACAUACGCCA	4	C4-7

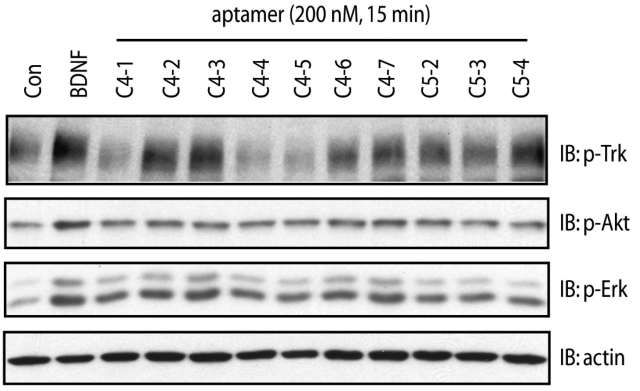

Fig. 3. Biochemical characterization of selected aptamers. Aptamers were synthesized by in vitro transcription and purified by acrylamide gel electrophoresis. Cortical neurons cultured from E18 rat pups were maintained in vitro for 12 to 14 days. Cortical neurons were incubated with vehicle, BDNF (10 ng/ml), or indicated aptamers (200 nM) for 15 min. Cell lysates were resolved onto SDS-PAGE. The blots were probed with indicated antibodies. The p-Trk antibody recognizes p-Trk pY816. Con, control; IB, immunoblotting.

effect of C4-3. Activation of TrkB by C4-3 was time-dependent (Fig. 6C); its peak activity was evident at 15 min and, like BDNF, waned after 2 h of incubation (Fig. 6C).

If C4-3 binds and activates TrkB per se in cortical neurons, knockdown of TrkB protein would be expected to reduce the agonistic activity of C4-3. We tested this idea with TrkB-shRNA-expressing lentiviral vectors (Huang et al., 2008). The expression of TrkB protein was largely reduced in TrkB-shRNA treated neurons (Huang et al., 2008) (Fig. 6D). Consistent with our prediction, knockdown of TrkB protein in cortical neurons resulted in reduced p-TrkB in both BDNF and C4-3-treated cortical neurons (Fig. 6D), thus further demonstrating that C4-3 specifically activates TrkB signaling in cultured neurons. In this experiment, we found the basal p-Trk level to be slightly increased in cells treated with the TrkB-shRNA lentivirus versus that of the control. This increase is possibly the result of the antibody cross-reacting with p-TrkC, which may have been up-regulated in response to the depletion of TrkB protein.

C4-3 Partially Inhibits BDNF-Mediated Activation of TrkB. Because both BDNF and C4-3 are able to bind and activate TrkB, we queried whether C4-3 and BDNF might have an additive or synergistic effect on TrkB signaling. To address this question, cortical neurons were preincubated with varying concentrations of C4-3 or scrambled aptamer for 15 min followed by brief incubation of BDNF. Of interest,

MOL PHARM
MOLECULAR PHARMACOLOGY
aspet
Downloaded from molpharm.aspetjournals.org at Universidade do Estado do Rio de Janeiro on December 1, 2012

MOL PHARM
MOLECULAR PHARMACOLOGY
aspet

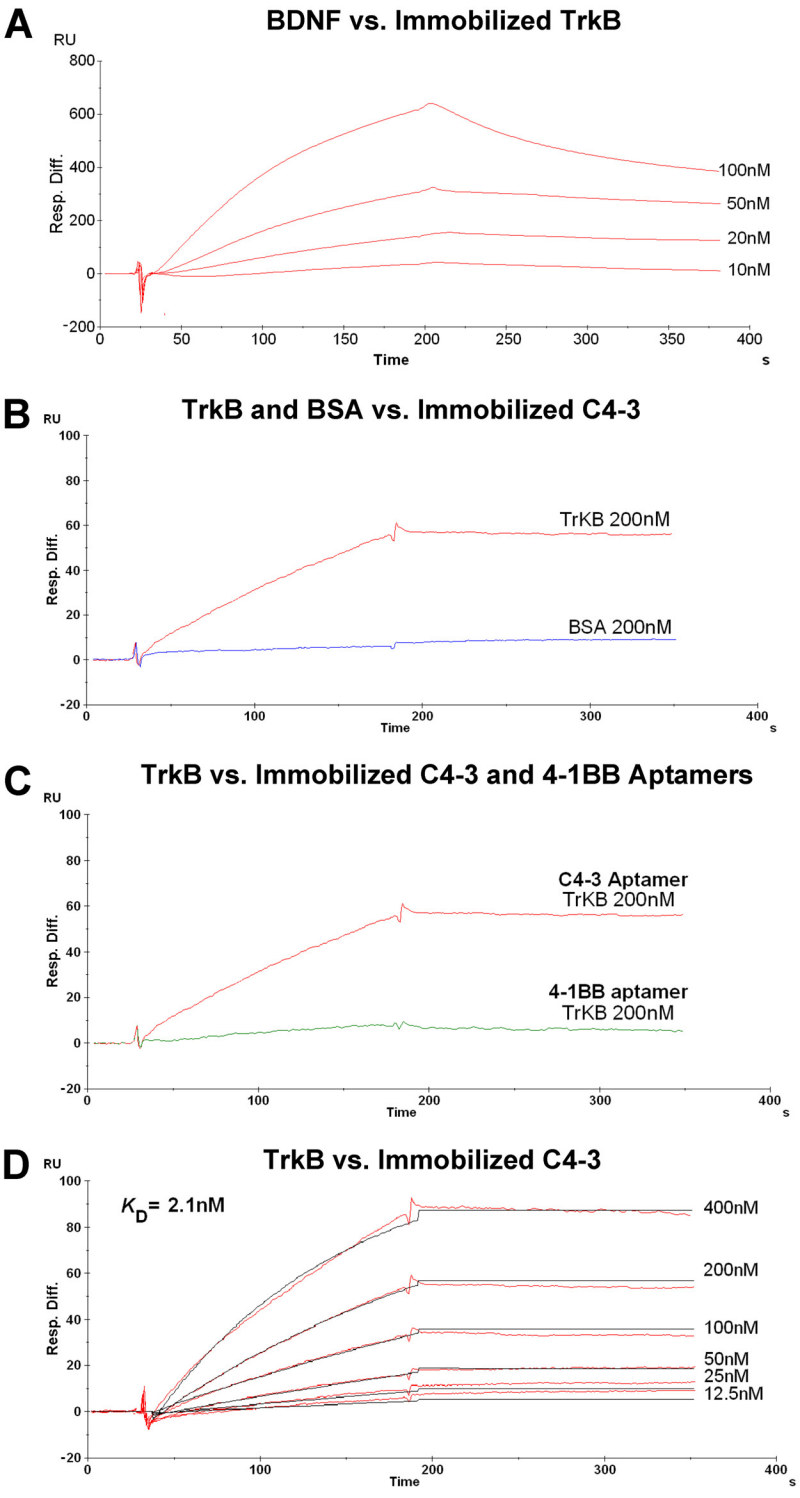

Fig. 4. SPR measurements of binding of C4-3 to TrkB protein in a cell-free system. A, the functionality of a recombinant murine TrkB extracellular domain was evaluated by passing four different concentrations of recombinant BDNF over the surface immobilized protein. B, interaction of recombinant murine TrkB extracellular domain [applied at 200 nM concentration (red trace)] with immobilized C4-3. Bovine serum albumin ([applied at 200 nM concentration (blue trace)] serves as a specificity control. C, application of 200 nM recombinant murine TrkB extracellular domain to immobilized C4-3 (red trace) or immobilized 4-1BB aptamer (green trace), which serves as a specificity control. D, high-affinity interaction between immobilized C4-3 aptamer and TrkB recombinant extracellular domain. Six different TrkB concentrations were analyzed (12.5–400 nM; data shown with red traces). A significant K_D value of 2.1 nM was determined using Langmuir fitting (shown with black lines) with mass transfer. RU, resonance units; Resp. Diff., response difference.

the BDNF-mediated increase of p-TrkB was attenuated by C4-3 in a concentration-dependent manner (Fig. 7A). The inhibition by C4-3 was dependent on the concentration of BDNF in that 2 ng/ml BDNF was inhibited more effectively than 5 ng/ml BDNF (Fig. 7A). This effect was specific to C4-3 because various concentrations of a scrambled aptamer did not inhibit BDNF-mediated activation of TrkB (Fig. 7B). It is noteworthy that the persistence of enhanced TrkB phosphorylation was evident even with the highest aptamer concentration (200 nM) coincubated with BDNF compared with vehicle (Fig. 7, A and B). Thus, in addition to the ability of C4-3 to activate TrkB signaling (Fig. 6), C4-3 can partially inhibit BDNF-mediated activation of TrkB in a concentration-dependent manner.

C4-3 Exerts Neuroprotective Effects on Cultured Cortical Neurons. Because reduced expression of BDNF is thought to contribute to death of CNS neurons in animal models of Huntington's disease and Alzheimer's disease, we asked whether C4-3 exhibits neuroprotective effects on cultured cortical neurons. For this experiment, we acutely with-

Downloaded from molpharm.aspetjournals.org at Universidade do Estado do Rio de Janeiro on December 1, 2012

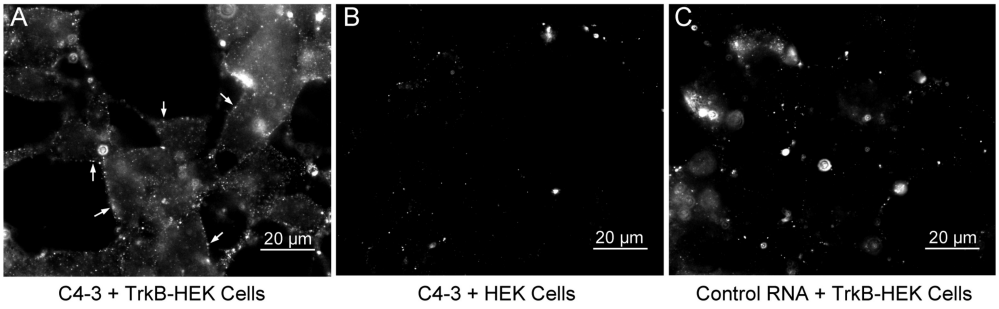

Fig. 5. C4-3 is specifically internalized by TrkB-expressing HEK cells. TrkB-expressing or TrkB-negative HEK cells were incubated with 100 nM FAM-labeled C4-3 or control RNA for 1 h at 37°C. Surface-bound RNA was stripped from the cells with a salt/acid wash, and then cells were fixed with formaldehyde, permeabilized, and labeled with anti-FAM and fluorescent secondary antibodies. A, TrkB-expressing HEK cells incubated with C4-3. B, HEK cells incubated with C4-3. C, TrkB-expressing HEK cells incubated with control RNA. Note evidence of C4-3 immunoreactivity signal within TrkB-expressing HEK cells [punctate (e.g., see arrows) and diffuse fluorescence in A] and signal absence in cells lacking TrkB (B). Signal detected with control RNA in TrkB-expressing HEK cells (C) provides a measure of nonspecific uptake of RNA molecules of the size of C4-3 in these cells.

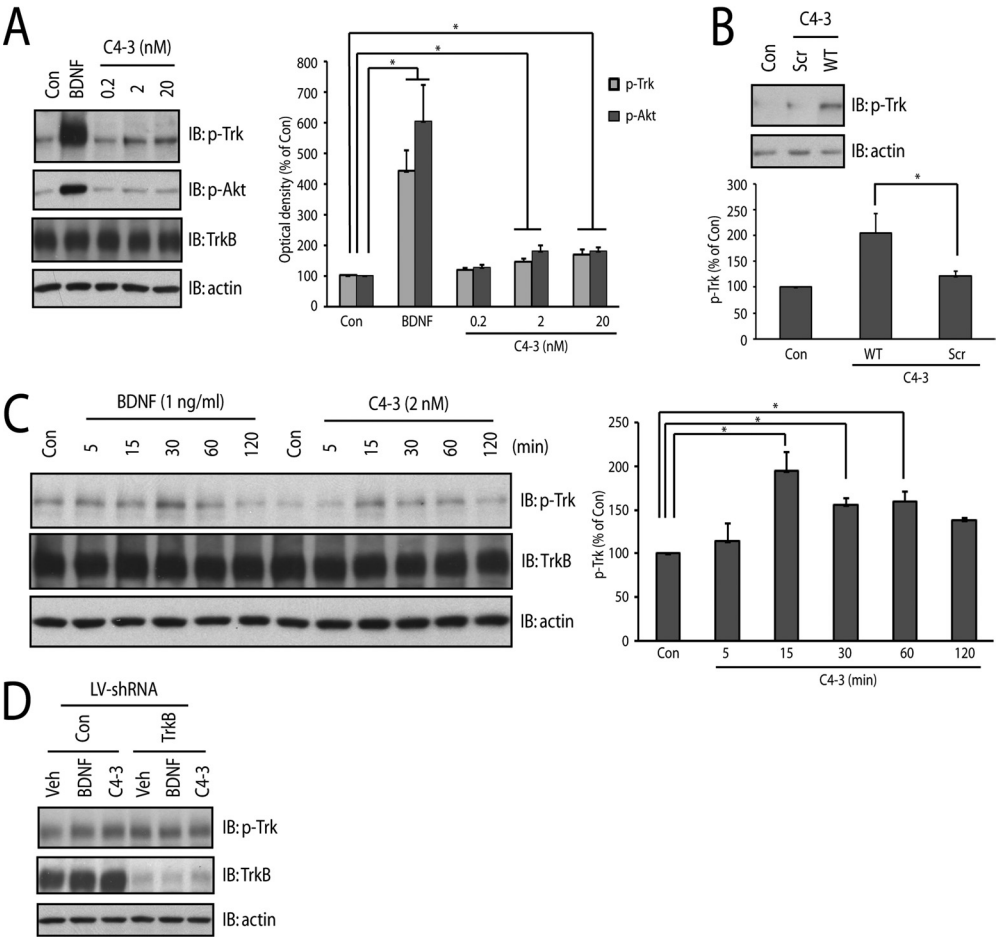

Fig. 6. C4-3 increases phosphorylation of Trk receptors in cultured neurons. C4-3 aptamers were chemically synthesized and purified by HPLC. Cortical neurons cultured from E18 rat pups were maintained in vitro for 12 to 14 days. Cell lysates were resolved with SDS-PAGE. A, a low nanomolar concentration of C4-3 was able to activate Trk receptors. Cortical neurons were incubated with vehicle, BDNF (10 ng/ml), or C4-3 with different concentrations for 15 min. B, C4-3, but not scrambled aptamer (variable region sequence of "Scr" is 5′-GACUAGCGAUCUGUUACGCA-3′) increased phosphorylation of Trk receptor. Cortical neurons were incubated with vehicle, C4-3, or scrambled aptamer (2 nM) for 15 min. C, C4-3 increased phosphorylation of Trk receptors in a time-dependent manner. Cortical neurons were incubated with vehicle, BDNF (1 ng/ml), or C4-3 (2 nM) for indicated periods of time. D, C4-3 induces phosphorylation of TrkB in a TrkB-requiring manner. Cortical neurons (days in vitro 6) were transduced with lentiviral vectors expressing either control or TrkB-shRNA and then maintained for additional 14 days. Cortical neurons were incubated with vehicle, BDNF (1 ng/ml), or C4-3 (2 nM) for 15 min. The p-Trk antibodies recognize p-Trk pY515 (in A, B, and C) or p-Trk pY816 (in D). Quantitative analyses of relative levels of *p*-Trk and *p*-Akt are shown in the bar graphs (number of experiments quantified includes 7 in A, 4 in B, and 5 in C). Statistical analyses were performed by one-way analysis of variance with post hoc test. $*$, $p < 0.05$. Con, control; IB, immunoblotting; WT, wild-type; Veh, vehicle.

drew the B27 growth supplement from healthy cultures of cortical neurons, which results in cell death that can be rescued by BDNF. Cells were protected from *N*-methyl-D-aspartate receptor activation-dependent toxicity by addition of 5*H*-dibenzo[*a*,*d*]cyclohepten-5,10-imine (MK-801) (1 μM) to the culture. After B27 withdrawal from the culture for

MOL PHARM
MOLECULAR PHARMACOLOGY
aspet
Downloaded from molpharm.aspetjournals.org at Universidade do Estado do Rio de Janeiro on December 1, 2012

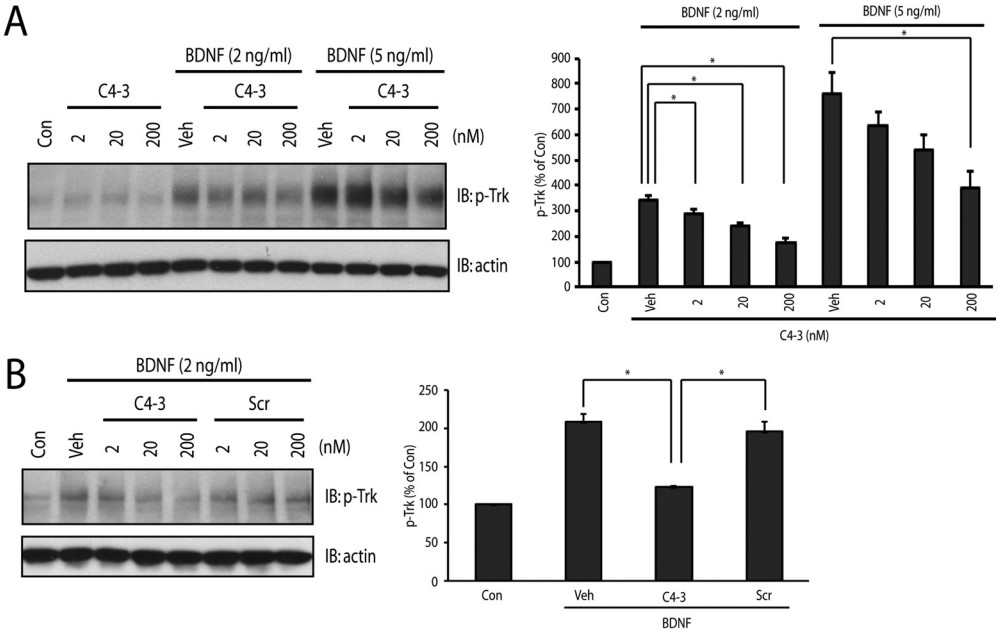

Fig. 7. C4-3 partially inhibits BDNF-induced phosphorylation of TrkB in cultured neurons. C4-3 or scrambled aptamer was chemically synthesized and purified by HPLC. Cortical neurons cultured from E18 rat pups were maintained in vitro for 12 to 14 days. Cell lysates were resolved with SDS-PAGE. A, C4-3 inhibited the phosphorylation of TrkB in a BDNF and C4-3 concentration-dependent manner. Cortical neurons were preincubated with vehicle or varying concentrations of C4-3 for 15 min and incubated for an additional 15 min in the presence of either vehicle or BDNF (2 or 5 ng/ml). B, C4-3, but not scrambled aptamer, reduced the phosphorylation of TrkB induced by BDNF. Cortical neurons were preincubated with vehicle, various concentrations of C4-3, or scrambled aptamer for 15 min and incubated for an additional 15 min in the presence of BDNF (2 ng/ml). The p-Trk blots were probed with p-Trk (pY515) (in A and B) antibody. Quantitative analyses of relative p-Trk levels are shown in the bar graphs ($n = 4$). Statistical analyses were performed by one-way analysis of variance with post hoc test. $*$, $p < 0.05$. Con, control; Veh, vehicle; IB, immunoblotting.

48 h, cell survival was assessed by measuring LDH release into the culture media (Lee and Chao, 2001). Neuronal cell death was induced upon B27 withdrawal (Fig. 8). Addition of BDNF (100 ng/ml) to the culture medium reduced cell death by approximately 40% (Fig. 8), confirming a previous report (Lee and Chao, 2001). Addition of C4-3 (2 nM) to the culture medium reduced cell death by 30%, whereas the scrambled aptamer was ineffective (Fig. 8), thereby demonstrating the prosurvival effects of C4-3 on CNS neurons.

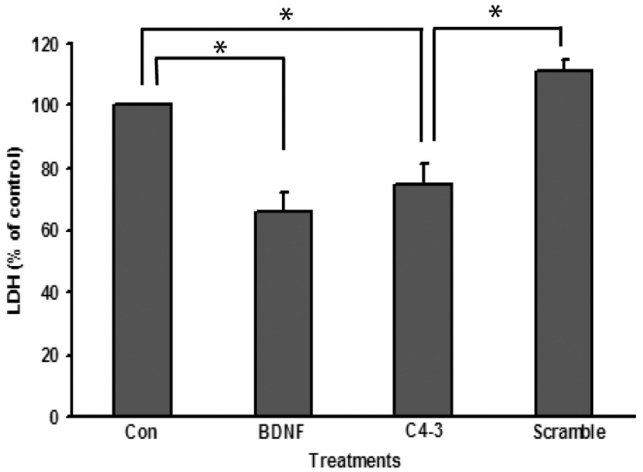

Fig. 8. C4-3 but not scrambled aptamer reduces neuronal cell death of cortical neurons in culture. Cortical neurons cultured from E18 rat pups were maintained in vitro for 12 to 14 days. Neuronal cell death was induced (day in vitro 10) by withdrawal of B27 for 72 h. Cortical neurons were treated with BDNF (100 ng/ml), C4-3 or scrambled aptamer (2 nM) every 24 h. LDH was measured at 72 h after treatments. The bar graph summarizes four independent experiments with six replicates for each treatment. The statistical analysis was performed with one way analysis of variance. $*$, $p < 0.05$.

Effects of C4-3 In Vivo. For a TrkB aptamer to have therapeutic utility, it must be able to activate TrkB in vivo. To determine whether C4-3 can activate TrkB in vivo, 2 μl of vehicle, C4-3 (2 μM), or scrambled aptamer (2 μM) was injected into the hippocampus of an adult mouse under isoflurane anesthesia. Thirty minutes after the onset of infusion, the animals were sacrificed and hippocampal homogenates were prepared. Lysates were resolved with SDS-PAGE followed by immunoblotting. Infusion of C4-3 but not of scrambled aptamer resulted in enhanced p-TrkB in hippocampus (Fig. 9A), thereby demonstrating TrkB agonistic activity of C4-3 in vivo.

The biochemical evidence that C4-3 can activate TrkB in vivo led us to seek the functional consequences of TrkB activation induced by C4-3 in vivo. This in turn led us to ask whether systemic treatment with C4-3 enhanced sensitivity to seizures evoked by the chemical convulsant, KA. That is, one consequence of enhanced TrkB activation in vivo is enhanced sensitivity to seizures evoked by kainic acid as evidenced by studies of mice with transgenic overexpression of either BDNF or TrkB (Croll et al., 1999; Lahteinen et al., 2003). To address this question, we used a model in which seizures were induced by direct injection of KA into the right amygdala of a wild-type mouse (Fig. 9B; see details under *Materials and Methods*). Fifteen minutes before infusion of KA was started, either C4-3 or a scrambled aptamer (200 nmol/kg) or vehicle alone was infused intravenously through the tail vein. Seizures were assessed by behavioral observation and electroencephalography, the latter detected with a bipolar recording electrode implanted in the dorsal hip-

MOL PHARM
MOLECULAR PHARMACOLOGY
aspet
Downloaded from molpharm.aspetjournals.org at Universidade do Estado do Rio de Janeiro on December 1, 2012

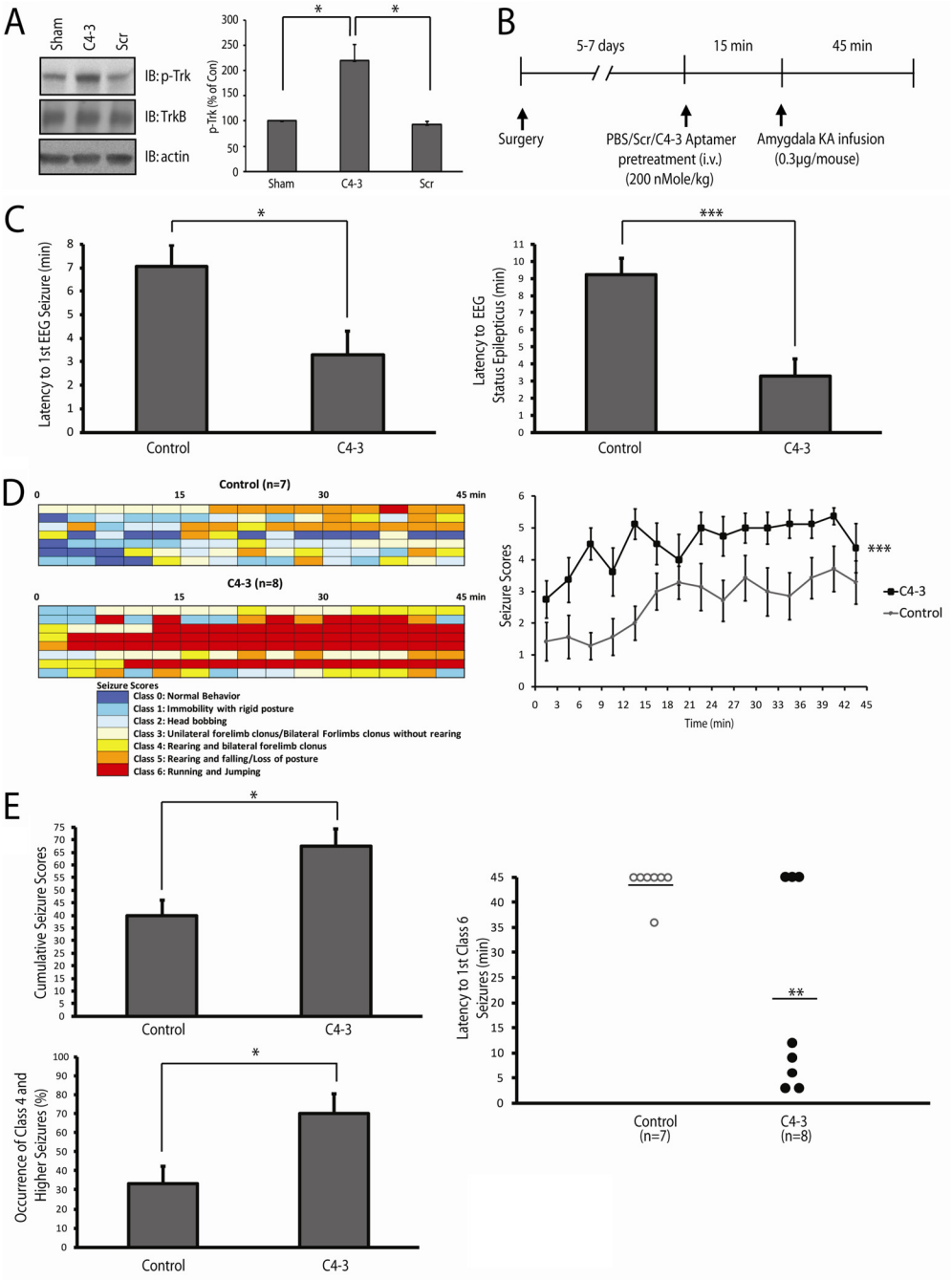

Fig. 9. C4-3 activates TrkB in vivo. A, infusion of C4-3 but not scrambled aptamer activates TrkB in vivo. Adult mice were anesthetized with isoflurane during infusion. Animals were awakened after completion of infusion. Mouse hippocampi were infused with 2 μl of vehicle, C4-3, or scrambled aptamer (2 μM in PBS, 0.1 μl/min) over a 20-min period. Thirty minutes after the onset of infusion, hippocampi were dissected, and tissue homogenates were prepared. Proteins were resolved with SDS-PAGE. The blots were probed with indicated antibodies. The p-Trk blots were probed with p-Trk (pY705/706) antibody. Quantitative analysis of relative p-Trk levels is shown in bar graph ($n = 3$). Statistical analyses were performed by one-way analysis of variance with post hoc test. *, $p < 0.05$. B, schematic diagram of experiment. Five to 7 days after surgery, either PBS or Scr aptamer or C4-3 aptamer (aptamers dissolved in PBS, 200 nmol/kg) was injected intravenously through tail vein 15 min before KA amygdala infusion. Both EEG and behavior were monitored for 45 min after infusion. The PBS ($n = 3$) and Scr aptamer ($n = 4$) groups were combined into a single control group ($n = 7$) compared with C4-3 ($n = 8$) because of the absence of a significant difference between them (Mann-Whitney U test or Student's t test, $p > 0.05$). C, C4-3 reduced the latency to onset of first electrographic seizure compared with control (left, Student's t test, *, $p < 0.05$) and the latency to onset of EEG status epilepticus, which is defined by continuous electrographic seizures including postictal depression and/or polyspikes (right, Student's t test, ***, $p < 0.001$). D, time course of seizure severity in each control or C4-3-pretreated animal (left, one mouse per row). The maximum seizure score of each animal was measured every 3 min over a 45-min period. The time scale in each box was 3 min. Note that blue boxes representing class 0 seizure-normal behavior were commonly found in the control group, whereas red boxes representing class 6 seizure-jumping and running were frequently observed in the C4-3-pretreated mice (left). Time course of average seizure scores evaluated every 3 min over a 45-min period (right, two-way analysis of variance, statistical significance was found between control and C4-3-pretreated groups, ***, $p < 0.001$). E, C4-3 increased the occurrence of class 4, 5, or 6 seizures (left lower) and cumulative seizure scores (left upper) compared with controls over a 45-min period (Student's t test, *, $p < 0.05$). C4-3 decreased the latency to class 6 seizures (right). ○, control ($n = 7$); ●, C4-3 ($n = 8$). Mann-Whitney U test, **, $p < 0.01$. IB, immunoblotting.

MOL PHARM
MOLECULAR PHARMACOLOGY
aspet
Downloaded from molpharm.aspetjournals.org at Universidade do Estado do Rio de Janeiro on December 1, 2012

MOL PHARM

MOLECULAR PHARMACOLOGY

pocampus contralateral to injection site. After infusion of PBS or scrambled aptamer through the tail vein, the initial electrographic seizure was detected 7.1 ± 0.9 min (n = 7) after completion of KA infusion into the amygdala (Fig. 9C, left panel); continuous electrographic seizures (status epilepticus) ensued shortly thereafter (9.2 ± 0.95 min; n = 7) (Fig. 9C, right panel). In contrast with controls, infusion of C4-3 via the tail vein 15 min before KA injection reduced both the latency to onset of the first EEG seizure (3.28 ± 1.02 min, n = 8) compared with that of the control (7.1 ± 0.9 min, n = 7; p = 0.0167, Student's t test) and EEG status epilepticus (3.28 ± 1.02 min, n = 8) compared with the control (9.2 ± 0.95 min, n = 7; p = 0.0009, Student's t test). Likewise, compared with controls, infusion of C4-3 caused enhanced behavioral seizure responses to KA. The number of animals exhibiting seizures of behavioral class 4 or higher was increased in C4-3-pretreated mice (70 ± 10%) compared with that of control mice (33 ± 9%) (Fig. 9E). Cumulative seizure scores during a period of 45 min after KA infusion were increased in C4-3-pretreated mice compared with controls (Fig. 9E). Whereas a single control mouse (1 of 7) exhibited the most severe seizure (class 6), the majority of C4-3 pretreated mice (5 of 8) exhibited class 6 seizures with shorter latency and longer duration (Fig. 9, D and E). Of importance, systemic infusion of C4-3 alone was not sufficient to induce seizures because infusion of C4-3 into the tail vein followed by infusion of vehicle into the amygdala did not induce seizures (not shown). Moreover, direct infusion of C4-3 (2 μM) into the amygdala was not sufficient to induce seizures as detected by behavioral or electrophysiological measures (not shown). In summary, these results demonstrate that C4-3 enhances sensitivity to KA-induced seizures, a predicted functional consequence of enhanced activation of TrkB in vivo.

Discussion

The objective of this study was to identify an RNA partial agonist for TrkB. Toward that end, we developed a novel cell internalization SELEX approach based on the understanding that TrkB is internalized after binding of neurotrophins and subsequent receptor activation. In this proof-of-concept study, aptamers selected with this cell-based functional screen were characterized with respect to their pharmacological, biochemical, and functional properties in vitro and in vivo. Several principal findings emerged. A subset of aptamers capable of activating TrkB signaling in cultured cortical neurons was identified. Characterization of one of these aptamers, C4-3, revealed that it bound the ectodomain of TrkB with high affinity (K_D ~2 nM) and potently and selectively activated TrkB signaling in cortical neurons. C4-3 also partially inhibited BDNF-mediated TrkB activation in cortical neurons, a property consistent with its classification as a partial agonist. C4-3 exerts neuroprotective effects in cortical neurons in vitro. Biochemical, electrophysiological, and behavioral measures indicate that C4-3 can activate TrkB in mouse brain in vivo. We conclude that C4-3 provides a potentially valuable therapeutic reagent for modulating activation of TrkB in diverse CNS disorders. Moreover this cell internalization SELEX approach may be broadly applicable for identifying aptamers with agonist, partial agonist, or antagonist properties for specific cell surface RTKs.

A Cell-Based Functional Screen for RTK RNA Agonists. RTKs play a critical role in cell signaling by conveying extracellular stimuli to intracellular signaling pathways. Many members of the large RTK family have been implicated as key regulators of various cellular processes in health and disease. RTKs have thus emerged as promising therapeutic targets for a number of nervous system disorders (Lemmon and Schlessinger, 2010). Therapeutic approaches that target RTKs for treatment of diverse diseases, including cancer and neurodegenerative diseases, have also been sought for many years.

A number of therapeutic agents targeting RTKs are in clinical use for treatment of cancer and other diseases (Lemmon and Schlessinger, 2010). These drugs are small molecules or monoclonal antibodies that bind the ectodomain of the RTK (Reichert and Valge-Archer, 2007). RNA aptamers represent an emerging class of therapeutic agents with some advantages over small molecule drugs and antibody-based therapeutic agents (Keefe et al., 2010). Whereas small molecule drugs often exhibit difficult-to-explain off-target effects, RNA aptamers exhibit specificities and affinities comparable with those of antibodies. The aptamer identification process is considerably less complex and expensive than that for small molecules because screening for aptamers is performed with a single complex mixture whereas each member of a (usually vast) small molecule library must be screened individually. In contrast to antibodies, aptamers can be produced economically with chemical synthesis, are amenable to chemical modification, and have low immunogenicity. The ability to recover and identify a subset of RNAs from a complex library that exhibits desirable properties (in addition to target binding) in aptamer screens is another property that sets the aptamer platform apart.

The potential applications for RTK-selective aptamers have led others to search for aptamers specific for particular RTKs, including HER3, RET, and Tie2 (Chen et al., 2003; Cerchia et al., 2005; White et al., 2008). Some of the aptamers that emerged from these selections exhibited antagonistic activity; however, aptamer agonists or partial agonists were not described. It is difficult to compare the outcomes of these selections with that for TrkB agonists described here. However, a plausible explanation for the absence of agonists from these screens is that incorporation of a functional component into aptamer screens may be necessary to sufficiently enrich for agonists.

For the TrkB aptamer selection, we sought to exploit the fact that RTK activation is usually followed by receptor/ligand cointernalization. By enriching for sequences that bound TrkB and were subsequently internalized, we expected to also enrich for sequences that activate the receptor. To identify the most prevalent sequences at a relatively early round of selection, we sequenced the selected pool with 454 sequencing technology, which yielded thousands of sequences. The functional activity of the selected aptamers was determined by measuring their impact on TrkB phosphorylation, a surrogate measure of TrkB activation. Of interest, the majority of the 13 RNAs chosen for this characterization exhibited TrkB agonistic activity in cultured neurons (Fig. 3A), thus demonstrating the efficiency of the functional aptamer selection.

C4-3 Is a Functional Ligand for TrkB. "Partial agonist" refers to a molecule that binds to a receptor and stabilizes a

Downloaded from molpharm.aspetjournals.org at Universidade do Estado do Rio de Janeiro on December 1, 2012

conformation less productive for activation than a full agonist. Surface plasmon resonance experiments demonstrated that C4-3 bound to the ectodomain of TrkB with high affinity (K_d ~2.1 nM) (Fig. 4). C4-3 activated TrkB signaling in cortical neurons, albeit less efficiently than the endogenous TrkB agonist, BDNF (Fig. 6, A and C). Moreover, coincubation of C4-3 with BDNF revealed a C4-3 concentration-dependent partial inhibition of BDNF-induced activation of TrkB (Fig. 7, A and B). Collectively, these findings support the idea that C4-3 binds TrkB and stabilizes a less productive conformation than BDNF and should thus be classified as a partial agonist. Of importance, binding of TrkB by either BDNF or C4-3 would be expected to induce its internalization, an event that could limit activation of TrkB by extracellular ligands. If, as seems likely, the extent of internalization of TrkB induced by BDNF and C4-3 is similar, then receptor internalization induced by C4-3 is not sufficient to account for the antagonist activity of C4-3.

The partial agonist activity of C4-3 proved sufficient to confer neuroprotective effects on cortical neurons in vitro. These effects were examined in cultures in which neuronal cell death was induced by B27 withdrawal from the culture medium. Addition of exogenous BDNF to these cultures prevented cell death (Fig. 8A), demonstrating that enhancing TrkB activation promotes neuronal survival under these conditions. Likewise, C4-3, but not scrambled aptamer, potently reduced cell death in these cultures (Fig. 8A), thereby demonstrating a neuroprotective effect of C4-3.

The evidence that C4-3 can selectively activate TrkB in cortical neurons and exert neuroprotective effects in vitro provided a strong rationale for determining whether C4-3 could activate TrkB in vivo. After direct infusion of C4-3 into mouse hippocampus in vivo, the p-Trk content was enhanced in hippocampal lysates in comparison with that in inactive controls (Fig. 9A), thus demonstrating the agonist activity of C4-3 in vivo. To obtain physiological evidence of C4-3-mediated activation of TrkB in vivo, we examined the effects of C4-3 on the development of seizures induced by intra-amygdala infusion of KA. We chose this model because increased TrkB activation in vivo enhances sensitivity to seizures evoked by KA as shown by studies of mice that overexpress BDNF or TrkB (Croll et al., 1999; Lahteinen et al., 2003). Indeed, systemically administered C4-3 enhances the sensitivity and severity of KA evoked seizures. The mechanism by which C4-3 gains access to the brain in the context of this experiment is uncertain. Seizure activity locally in the kainate-infused amygdala may have resulted in transient breakdown of the blood-brain barrier and promoted access of C4-3 before emergence of behavioral seizures or EEG seizures detected in the contralateral hippocampus. Of importance, seizures were not elicited upon systemic administration of C4-3 when vehicle was infused into amygdala or with direct infusion of C4-3 into amygdala (not shown), thus demonstrating that C4-3 alone does not elicit seizures. Taken together, these results suggest that C4-3 is a selective partial agonist of TrkB, which confers neuroprotective effects in vitro and activates TrkB in vivo.

Advantages of TrkB Partial Agonists as Therapeutic Reagents. TrkB has emerged as a promising therapeutic target for a variety of diseases including neurodegenerative disorders. For instance, reduced expression of BDNF is thought to contribute to degeneration of striatal neurons in Huntington's disease (Zuccato et al., 2001). Moreover, BDNF levels are reduced in the entorhinal cortex and hippocampus of patients with Alzheimer's disease (Narisawa-Saito et al., 1996; Hock et al., 2000). Neuronal degeneration in these brain regions is a signature of Alzheimer's disease. Furthermore, increasing the levels of BDNF in the entorhinal cortex in rodent and primate models of Alzheimer's disease has a neuroprotective effect and improves cognitive function (Nagahara et al., 2009). Whereas these and other data provide a strong rationale for the pursuit of TrkB agonists as therapeutic agents for Alzheimer's disease, the present lack of optimal TrkB agonists for therapeutic applications presents an obstacle for such endeavors. Use of BDNF for therapeutic applications is limited by its side effects (Ochs et al., 2000), which may result from the overactivation of TrkB (because of the additive concentrations of endogenous and exogenous BDNF) in nondiseased cells. Indeed, excessive activation of TrkB signaling in CNS neurons has deleterious consequences, including epilepsy and neuropathic pain (Croll et al., 1999; Lahteinen et al., 2003; Coull et al., 2005; Hu and Russek, 2008; He et al., 2010). Although several classes of artificial TrkB agonists have been developed, including peptide mimetics (O'Leary and Hughes, 2003), monoclonal antibodies (Qian et al., 2006), and diverse small molecules (Jang et al., 2010; Massa et al., 2010), these reagents seem to be full agonists and thus may have the same drawbacks as BDNF.

These considerations led us to seek TrkB partial agonists, which would activate submaximal TrkB signaling while capping maximal activation levels (Tsai, 2007). The functional cell-based SELEX approach described herein permitted identification of C4-3, an aptamer that exhibits TrkB partial agonistic activity and neuroprotective effects in vitro and lacks unwanted seizure-inducing actions in vivo. Thus, C4-3 may prove to be a valuable reagent that can tilt the balance of TrkB signaling to a level with beneficial effects, yet prevent excessive activation of TrkB. Future studies will seek beneficial effects of C4-3 in mouse models of neurodegenerative disorders.

Acknowledgments

We thank Dr. James O. McNamara, Sr., for many in depth discussions of this work and for critical feedback on the manuscript, Dr. William Thiel for critical feedback on the manuscript, and Georgia Alexander for technical assistance with aptamer brain infusions.

Authorship Contributions

Participated in research design: Huang, Hernandez, Giangrande, and McNamara.

Conducted experiments: Huang, Hernandez, Gu, Stockdale, and McNamara.

Contributed new reagents or analytic tools: Stockdale, Nanapaneni, Scheetz, Behlke, Peek, Bair, Giangrande, and McNamara.

Performed data analysis: Huang, Hernandez, Gu, Stockdale, Nanapaneni, Scheetz, Bair, and McNamara.

Wrote or contributed to the writing of the manuscript: Huang and McNamara.

References

Cerchia L, Ducongé F, Pestourie C, Boulay J, Aissouni Y, Gombert K, Tavitian B, de Franciscis V, and Libri D (2005) Neutralizing aptamers from whole-cell SELEX inhibit the RET receptor tyrosine kinase. *PLoS Biol* **3:**e123.

Chen CH, Chernis GA, Hoang VQ, and Landgraf R (2003) Inhibition of heregulin signaling by an aptamer that preferentially binds to the oligomeric form of human epidermal growth factor receptor-3. *Proc Natl Acad Sci USA* **100:**9226–9231.

Coull JA, Beggs S, Boudreau D, Boivin D, Tsuda M, Inoue K, Gravel C, Salter MW,

MOL PHARM
MOLECULAR PHARMACOLOGY
aspet
Downloaded from molpharm.aspetjournals.org at Universidade do Estado do Rio de Janeiro on December 1, 2012

and De Koninck Y (2005) BDNF from microglia causes the shift in neuronal anion gradient underlying neuropathic pain. *Nature* **438:**1017–1021.
Croll SD, Suri C, Compton DL, Simmons MV, Yancopoulos GD, Lindsay RM, Wiegand SJ, Rudge JS, and Scharfman HE (1999) Brain-derived neurotrophic factor transgenic mice exhibit passive avoidance deficits, increased seizure severity and in vitro hyperexcitability in the hippocampus and entorhinal cortex. *Neuroscience* **93:**1491–1506.
He XP, Pan E, Sciarretta C, Minichiello L, and McNamara JO (2010) Disruption of TrkB-mediated phospholipase Cγ signaling inhibits limbic epileptogenesis. *J Neurosci* **30:**6188–6196.
Hernandez FJ, Dondapati SK, Ozalp VC, Pinto A, O'Sullivan CK, Klar TA, and Katakis I (2009a) Label free optical sensor for Avidin based on single gold nanoparticles functionalized with aptamers. *J Biophotonics* **2:**227–231.
Hernandez FJ, Kalra N, Wengel J, and Vester B (2009b) Aptamers as a model for functional evaluation of LNA and 2′-amino LNA. *Bioorg Med Chem Lett* **19:**6585–6587.
Hock C, Heese K, Hulette C, Rosenberg C, and Otten U (2000) Region-specific neurotrophin imbalances in Alzheimer disease: decreased levels of brain-derived neurotrophic factor and increased levels of nerve growth factor in hippocampus and cortical areas. *Arch Neurol* **57:**846–851.
Hu Y and Russek SJ (2008) BDNF and the diseased nervous system: a delicate balance between adaptive and pathological processes of gene regulation. *J Neurochem* **105:**1–17.
Huang EJ and Reichardt LF (2001) Neurotrophins: roles in neuronal development and function. *Annu Rev Neurosci* **24:**677–736.
Huang YZ, Pan E, Xiong ZQ, and McNamara JO (2008) Zinc-mediated transactivation of TrkB potentiates the hippocampal mossy fiber-CA3 pyramid synapse. *Neuron* **57:**546–558.
Huang YZ and McNamara JO (2010) Mutual regulation of Src family kinases and the neurotrophin receptor TrkB. *J Biol Chem* **285:**8207–8217.
Institute of Laboratory Animal Resources (1996) *Guide for the Care and Use of Laboratory Animals*, 7th ed. Institute of Laboratory Animal Resources, Commission on Life Sciences, National Research Council, Washington DC.
Jang SW, Liu X, Yepes M, Shepherd KR, Miller GW, Liu Y, Wilson WD, Xiao G, Blanchi B, Sun YE, et al. (2010) A selective TrkB agonist with potent neurotrophic activities by 7,8-dihydroxyflavone. *Proc Natl Acad Sci USA* **107:**2687–2692.
Jorenby DE, Hays JT, Rigotti NA, Azoulay S, Watsky EJ, Williams KE, Billing CB, Gong J, Reeves KR, and Varenicline Phase 3 Study Group (2006) Efficacy of varenicline, an $\alpha4\beta2$ nicotinic acetylcholine receptor partial agonist, vs placebo or sustained-release bupropion for smoking cessation: a randomized controlled trial. *JAMA* **296:**56–63.
Keefe AD, Pai S, and Ellington A (2010) Aptamers as therapeutics. *Nat Rev Drug Discov* **9:**537–550.
Lähteinen S, Pitkänen A, Koponen E, Saarelainen T, and Castrén E (2003) Exacerbated status epilepticus and acute cell loss, but no changes in epileptogenesis, in mice with increased brain-derived neurotrophic factor signaling. *Neuroscience* **122:**1081–1092.
Lee FS and Chao MV (2001) Activation of Trk neurotrophin receptors in the absence of neurotrophins. *Proc Natl Acad Sci USA* **98:**3555–3560.
Lemmon MA and Schlessinger J (2010) Cell signaling by receptor tyrosine kinases. *Cell* **141:**1117–1134.
Massa SM, Yang T, Xie Y, Shi J, Bilgen M, Joyce JN, Nehama D, Rajadas J, and Longo FM (2010) Small molecule BDNF mimetics activate TrkB signaling and prevent neuronal degeneration in rodents. *J Clin Invest* **120:**1774–1785.
McNamara JO, Kolonias D, Pastor F, Mittler RS, Chen L, Giangrande PH, Sullenger B, and Gilboa E (2008) Multivalent 4-1BB binding aptamers costimulate CD8+ T cells and inhibit tumor growth in mice. *J Clin Invest* **118:**376–386.
Mouri G, Jimenez-Mateos E, Engel T, Dunleavy M, Hatazaki S, Paucard A, Matsushima S, Taki W, and Henshall DC (2008) Unilateral hippocampal CA3-predominant damage and short latency epileptogenesis after intra-amygdala microinjection of kainic acid in mice. *Brain Res* **1213:**140–151.
Nagahara AH, Merrill DA, Coppola G, Tsukada S, Schroeder BE, Shaked GM, Wang L, Blesch A, Kim A, Conner JM, et al. (2009) Neuroprotective effects of brain-derived neurotrophic factor in rodent and primate models of Alzheimer's disease. *Nat Med* **15:**331–337.
Narisawa-Saito M, Wakabayashi K, Tsuji S, Takahashi H, and Nawa H (1996) Regional specificity of alterations in NGF, BDNF and NT-3 levels in Alzheimer's disease. *Neuroreport* **7:**2925–2928.
Ochs G, Penn RD, York M, Giess R, Beck M, Tonn J, Haigh J, Malta E, Traub M, Sendtner M, et al. (2000) A phase I/II trial of recombinant methionyl human brain derived neurotrophic factor administered by intrathecal infusion to patients with amyotrophic lateral sclerosis. *Amyotroph Lateral Scler Other Motor Neuron Disord* **1:**201–206.
O'Leary PD and Hughes RA (2003) Design of potent peptide mimetics of brain-derived neurotrophic factor. *J Biol Chem* **278:**25738–25744.
Qian MD, Zhang J, Tan XY, Wood A, Gill D, and Cho S (2006) Novel agonist monoclonal antibodies activate TrkB receptors and demonstrate potent neurotrophic activities. *J Neurosci* **26:**9394–9403.
Qin PZ and Pyle AM (1999) Site-specific labeling of RNA with fluorophores and other structural probes. *Methods* **18:**60–70.
Racine RJ (1972) Modification of seizure activity by electrical stimulation. II. Motor seizure. *Electroencephalogr Clin Neurophysiol* **32:**281–294.
Reichert JM and Valge-Archer VE (2007) Development trends for monoclonal antibody cancer therapeutics. *Nat Rev Drug Discov* **6:**349–356.
Robinson DS, Rickels K, Feighner J, Fabre LF Jr, Gammans RE, Shrotriya RC, Alms DR, Andary JJ, and Messina ME (1990) Clinical effects of the 5-HT1A partial agonists in depression: a composite analysis of buspirone in the treatment of depression. *J Clin Psychopharmacol* **10:**67S–76S.
Scheetz TE, Trivedi N, Pedretti KT, Braun TA, and Casavant TL (2005) Gene transcript clustering: a comparison of parallel approaches. *Fut Gen Comput Sys* **21:**731–735.
Tsai SJ (2007) TrkB partial agonists: potential treatment strategy for major depression. *Med Hypotheses* **68:**674–676.
White RR, Roy JA, Viles KD, Sullenger BA, and Kontos CD (2008) (2008) A nuclease-resistant RNA aptamer specifically inhibits angiopoietin-1-mediated Tie2 activation and function. *Angiogenesis* **11:**395–401.
Whitney KD and McNamara JO (2000) GluR3 autoantibodies destroy neural cells in a complement-dependent manner modulated by complement regulatory proteins. *J Neurosci* **20:**7307–7316.
Zuccato C and Cattaneo E (2009) Brain-derived neurotrophic factor in neurodegenerative diseases. *Nat Rev Neurol* **5:**311–322.
Zuccato C, Ciammola A, Rigamonti D, Leavitt BR, Goffredo D, Conti L, MacDonald ME, Friedlander RM, Silani V, Hayden MR, et al. (2001) Loss of huntingtin-mediated BDNF gene transcription in Huntington's disease. *Science* **293:**493–498.

Address correspondence to: Dr. James O. McNamara II, Department of Internal Medicine, University of Iowa, 375 Newton Rd., Room 5204 MERF, Iowa City, IA 52242. E-mail: james-mcnamara@uiowa.edu

MOL PHARM
MOLECULAR PHARMACOLOGY
aspet
Downloaded from molpharm.aspetjournals.org at Universidade do Estado do Rio de Janeiro on December 1, 2012